AIAA JOURNAL
Vol. 41, No. 6, June 2003

Multiple-Timescale Analysis for Bifurcation from a Multiple-Zero Eigenvalue

Angelo Luongo* and Angelo Di Egidio†
Università di L'Aquila, 67040 L'Aquila, Italy
and
Achille Paolone‡
University of Rome "La Sapienza," 00184 Rome, Italy

Multiple-zero bifurcation of a general multiparameter dynamic system is analyzed using the multiple-scale method and exploiting the close similarities with eigensolution analysis for defective systems. Because of the coalescence of the eigenvalues, the Jacobian matrix at the bifurcation is nilpotent. This entails using timescales with fractional powers of the perturbation parameter. The reconstitution method is employed to obtain an ordinary differential equation of order equal to the algebraic multiplicity of the zero eigenvalue, in the unique unknown amplitude. When the algorithm is applied to a double-zero eigenvalue, Bogdanova–Arnold's normal form for the bifurcation equation is recovered. A detailed step-by-step algorithm is described for a general system to obtain the numerical coefficients of the relevant bifurcation equation. The mechanical behavior of a nonconservative two-degree-of-freedom system is studied as an example.

Nomenclature

a = time-dependent amplitude of motion
$\mathcal{C}$ = homoclinic boundary
$\mathcal{D}$ = divergence boundary
d_k = time-differential operator with respect to the time t_k
$\boldsymbol{F}$ = vector field
$\boldsymbol{F}_x^0$ = Jacobian matrix
$\mathcal{H}$ = Hopf boundary
m = codimension of the bifurcation and number of the control parameters
N = state-space dimension
$\mathcal{N}$ = nilpotent system locus
O = bifurcation point
t = time
t_k = kth slow time
$\boldsymbol{u}_k$ = generalized right eigenvectors of $\boldsymbol{F}_x^0$ where $k = 2, 3, \dots, m$
$\boldsymbol{u}_1$ = proper right eigenvector of $\boldsymbol{F}_x^0$
$\boldsymbol{v}_k$ = generalized left eigenvectors of $\boldsymbol{F}_x^0$ where $k = m, m-1, \dots, 2$
$\boldsymbol{v}_m$ = proper left eigenvector of $\boldsymbol{F}_x^0$
$\boldsymbol{w}$ = eigenvector of a perturbed matrix
$\boldsymbol{x}$ = vector of the state variables
δ_{jk} = Kronecker symbol, 0 if $j \neq k$, $\delta_{jj} = 1$
ε = perturbation parameter
κ = unfolding parameter
λ_i = high-order sensitivity of the eigenvalue λ_0, where $i > 0$
λ_0 = eigenvalue of $\boldsymbol{F}_x^0$ with algebraic multiplicity equal to m
$\boldsymbol{\mu}$ = control parameter vector
ξ = unfolding parameter

Subscripts

x = differentiation with respect to $\boldsymbol{x}$
μ = differentiation with respect to $\boldsymbol{\mu}$

Superscripts

0 = evaluation at $(\boldsymbol{x}, \boldsymbol{\mu}) = (\boldsymbol{0}, \boldsymbol{0})$
$\cdot$ = differentiation with respect to t

I. Introduction

THE multiple-timescale method has been widely used to analyze the dynamic response of weak nonlinear mechanical systems in both free and forced oscillation regimes.[1] As in other reduction methods, the multiple-timescale method transforms analysis of the evolution of a multidimensional dynamic system into that of an equivalent system of a dimension smaller than the original one and equal to its codimension.[2] The multiple-timescale method often implies a smaller computational effort than other reduction methods. Within bifurcation analysis, the main advantage of the method is the possibility of obtaining reduced equations without describing the center manifold in advance or expressing the Jacobian matrix at the critical state in Jordan form. As a result, bifurcation equations are obtained directly in normal form. Their coefficients are expressed in closed form in terms of the derivatives of the original vector field evaluated at the critical state, in a manner similar to the theory of static bifurcation of conservative systems.[3–6]

In the past, the method has been successfully applied by the authors to analyze nonresonant codimension-two bifurcations of the Hopf–Hopf and Hopf-divergence types (see Refs. 7 and 8) and the resonant codimension-three bifurcation of the Hopf–Hopf type (see Ref. 9). However, problems arise when the system's Jacobian matrix is nilpotent at the bifurcation point. In these cases, the classical method fails, and a nonstandard analysis must be performed. This requires the use of timescales with suitable fractional powers of the perturbation parameter, similar to the procedure employed in the eigenvalue sensitivity analysis of nilpotent matrices.[10–12] The method is illustrated here with reference to a general dynamic system undergoing a static bifurcation of codimension m for which, in the generic case, the Jacobian matrix contains a Jordan block of dimension m. The problem is believed to be new because methods in the literature typically refer to $m = 2$ or 3. The algorithm is successively adapted for $m = 2$, for which preliminary results were presented in Ref. 13. This codimension-two problem has already been

Received 6 September 2002; revision received 22 January 2003; accepted for publication 24 January 2003.

*Professor, Dipartimento di Ingegneria delle Strutture delle Acque e del Terreno, Monteluco di Roio; luongo@ing.univaq.it.

†Assistant Professor, Dipartimento di Ingegneria delle Strutture delle Acque e del Terreno, Monteluco di Roio; ade@ing.univaq.it.

‡Associate Professor, Dipartimento di Ingegneria Strutturale e Geotecnica, via Eudossiana 18; achille.paolone@uniroma1.it.

studied in the literature but only for a specific system[14,15]; the analysis was, moreover, limited to the first-order approximation, whereas the present paper considers higher-order approximations. The objective is achieved in two steps: first, several timescales with fractional powers of the perturbation parameter are introduced and solvability equations are obtained for the different orders. Subsequently, the real timescale and solvability equations are reconstituted.[16] When the proposed perturbative procedure is applied to the codimension-two problem, the resulting bifurcation equations are expressed directly in Bogdanova–Arnold's normal form (see Ref. 17).

An application of the procedure is finally presented to analyze the postcritical behavior of a double pendulum with elastic supports, loaded by a follower force.

II. Multiple-Zero Eigenvalue Analysis

A dynamic system is considered, having equations of motion

$$\dot{\boldsymbol{x}} = \boldsymbol{F}(\boldsymbol{x}, \boldsymbol{\mu}) \tag{1}$$

where $\boldsymbol{x} \in \mathbb{R}^N$ and $\boldsymbol{\mu} \in \mathbb{R}^m$. It is assumed that Eqs. (1) have been reduced to the so-called local form, so that they admit the trivial solution $\boldsymbol{x} = \boldsymbol{0}$, $\forall \boldsymbol{\mu}$. Let us further assume that $O := (\boldsymbol{x}, \boldsymbol{\mu}) = (\boldsymbol{0}, \boldsymbol{0})$ is a codimension-m bifurcation point, at which the Jacobian $\boldsymbol{F}_x^0 := \boldsymbol{F}_x(\boldsymbol{0}, \boldsymbol{0})$ admits one eigenvalue $\lambda_0 = 0$ with algebraic multiplicity $m > 1$, whereas the remaining eigenvalues are stable. In the generic case, only one critical eigenvector $\boldsymbol{u}$ exists associated with λ_0, so that the matrix $\boldsymbol{F}_x^0$ has an incomplete set of eigenvectors (defective matrix). A chain of m generalized (right) eigenvectors can be built up to complete the base, by recursively solving the following equations:

$$\left(\boldsymbol{F}_x^0 - \lambda_0 \boldsymbol{I}\right)\boldsymbol{u}_k = \boldsymbol{u}_{k-1}, \qquad k = 2, 3, \ldots, m \tag{2}$$

where $\boldsymbol{u}_1 \equiv \boldsymbol{u}$. A complete base of generalized left eigenvectors can also be found by recursively solving the following equations:

$$\left(\boldsymbol{F}_x^0 - \lambda_0 \boldsymbol{I}\right)^T \boldsymbol{v}_{j-1} = \boldsymbol{v}_j, \qquad j = m, m-1, \ldots, 2 \tag{3}$$

The left and right eigenvectors satisfy the following orthonormalization properties: $\boldsymbol{v}_j^T \boldsymbol{u}_k = \delta_{jk}$. This means that all of the eigenvectors $\boldsymbol{u}_k$ of the chain, except the higher-order eigenvector $\boldsymbol{u}_m$, belong to the range of the operator $\boldsymbol{F}_x^0 - \lambda_0 \boldsymbol{I}$, whereas $\boldsymbol{u}_m$ is external to it.

The aim of the analysis is to investigate the dynamics of the nonlinear system around the bifurcation point by applying a perturbation method. However, the orthogonality properties just recalled are responsible for the failure of the standard perturbation method, based on integer power series expansion of the perturbation parameter. The problem is addressed in the framework of eigenvalue sensitivity analysis,[10,11] which has strong analogies with the bifurcation analysis performed here. Therefore, it is worth summarizing the main steps of that procedure.

A. Eigenpair Sensitivity Analysis

Let $\boldsymbol{x}_E = \boldsymbol{x}_E(\boldsymbol{\mu})$ be an equilibrium path (not necessarily the trivial one) passing through the bifurcation point. Let us determine an asymptotic expression for the eigensolutions $[\boldsymbol{\lambda} = \boldsymbol{\lambda}(\boldsymbol{\mu}), \boldsymbol{w} = \boldsymbol{w}(\boldsymbol{\mu})]$ along the path, that is, let us solve the following eigenvalue problem:

$$\{\boldsymbol{F}_x[\boldsymbol{x}_E(\boldsymbol{\mu}), \boldsymbol{\mu}] - \lambda(\boldsymbol{\mu})\}\boldsymbol{w}(\boldsymbol{\mu}) = \boldsymbol{0} \tag{4}$$

asymptotically for $\boldsymbol{\mu} \to \boldsymbol{0}$. Let us decide to vary the control parameters $\boldsymbol{\mu}$ proportionally to ε, namely, $\boldsymbol{\mu} = \varepsilon\hat{\boldsymbol{\mu}}$, with $\hat{\boldsymbol{\mu}} = \mathcal{O}(1)$, so that $\boldsymbol{F}_x = \boldsymbol{F}_x(\varepsilon)$, $\lambda = \lambda(\varepsilon)$, and $\boldsymbol{w} = \boldsymbol{w}(\varepsilon)$. From a geometric point of view, the choice corresponds to spanning the neighborhood of the bifurcation point by straight lines. When $\boldsymbol{F}_x(\varepsilon)$ is expanded in series about the bifurcation point, Eq. (4) is

$$[(\boldsymbol{A}_0 + \varepsilon\boldsymbol{A}_1 + \cdots) - \lambda(\varepsilon)]\boldsymbol{w}(\varepsilon) = \boldsymbol{0} \tag{5}$$

in which $\boldsymbol{A}_0 := \boldsymbol{F}_x^0$ and $\boldsymbol{A}_1 := \boldsymbol{F}_{xx}^0(\mathrm{d}\boldsymbol{x}_E/\mathrm{d}\boldsymbol{\mu})_0 + \boldsymbol{F}_{x\mu}^0$. When the fractional power series expansion in Eqs. (A1a) and (A1b) of Appendix A are used, the perturbation equations in Eqs. (A2a–A2e) are then drawn. Equation (A2a) admits the eigenpair $(\lambda_0, \boldsymbol{w}_0) = (0, \boldsymbol{u}_1)$; Eq. (A2b) can be solved for any λ_1 because its known term $\boldsymbol{u}_1$ belongs to the range of the operator [see Eq. (A3b)] with λ_1 still being indeterminate. Similarly, Eq. (A2c) admits solution (A3c), with arbitrary λ_1 and λ_2, and so on. In proceeding to higher orders, a solvability condition is first required at the ε order, where the highest element of the chain $\boldsymbol{u}_m$ appears together with the perturbation $\boldsymbol{A}_1\boldsymbol{u}_1$. When orthogonality to $\boldsymbol{v}_m$ is required, the nonlinear equation (A4a) is drawn, from which m roots are found (first-order sensitivities of the m coincident eigenvalues λ_0). At higher orders, in contrast, linear equations of the type (A4b) and (A4c) are found, from which one value of $\lambda_2, \lambda_3, \ldots$ is drawn for each of the m first-order sensitivities. The coefficients of series (A1) are thus evaluated.

It can be seen that the left members of the solvability equations (A4) are monomials resulting from the expansion of the mth power of $\lambda - \lambda_0 \equiv \lambda$. Therefore, it seems convenient to combine all of the solvability conditions in a single algebraic equation of degree m [Eq. (A5)]. This equation can be referred to as the reconstituted sensitivity equation, according to the procedure commonly used in the multiple-scale method.[2,16] The sensitivity of the m-zero eigenvalue is, thus, governed by an algebraic equation of the mth degree. The reconstituted equation makes it possiblt to avoid the drawbacks that occur when $\lambda_1 \to 0$ for which the ordering in Eqs. (A1) is incorrect. These singular perturbations are always encountered if the whole neighborhood of the bifurcation point has to be spanned.[11] In contrast, the reconstituted sensitivity equation correctly furnishes $\lambda = \mathcal{O}(\varepsilon^{1/m})$, if $c_m = \mathcal{O}(\varepsilon)$ and $\lambda > \mathcal{O}(\varepsilon^{1/m})$, if $c_m < \mathcal{O}(\varepsilon)$.

B. Bifurcation Analysis

The bifurcation analysis is formally similar to the sensitivity analysis. Indeed, if the equations of motion (4) are expanded and written in the form

$$\left[\boldsymbol{F}_x^0 + \tfrac{1}{2}\left(\boldsymbol{F}_{xx}^0\hat{\boldsymbol{x}} + \boldsymbol{F}_{x\mu}^0\boldsymbol{\mu}\right)\varepsilon + \tfrac{1}{6}\left(\boldsymbol{F}_{xxx}^0\hat{\boldsymbol{x}}^2 + \cdots\right)\varepsilon^2 - D\right]\hat{\boldsymbol{x}} = \boldsymbol{0} \tag{6}$$

where the change of variable $\boldsymbol{x} \to \varepsilon\hat{\boldsymbol{x}}$ has been introduced and $D = \mathrm{d}/\mathrm{d}t$ is posed, then Eq. (6) is formally equal to the perturbed eigenvalue problem (5) in which λ is substituted by the operator D. The analogy suggests the expedience of introducing fractional power expansion of $\varepsilon^{1/m}$ for both the eigenvector $\boldsymbol{x}$ and the eigenvalue D, given in Appendix A by Eqs. (A1a′) and (A1b′), where a return to $\boldsymbol{x}$ is made. The formal series expansion of $\mathrm{d}/\mathrm{d}t$ corresponds to the introduction of the following fractional timescales:

$$t_0 = t, \qquad t_1 = \varepsilon^{1/m}t, \qquad t_2 = \varepsilon^{2/m}t, \ldots \tag{7}$$

with $d_k := \partial/\partial t_k$, $k = 1, 2, \ldots$. The bifurcation parameters are scaled as $\boldsymbol{\mu} = \varepsilon\hat{\boldsymbol{\mu}}$, so that the lowest-order derivative $\boldsymbol{F}_{x\mu}^0\boldsymbol{x}_0\hat{\boldsymbol{\mu}}$ appears at the same level as the resonant term $\boldsymbol{F}_{xx}^0\boldsymbol{x}_0^2$. The perturbation equations (A2a′–A2e′) are obtained. Because a unique real critical eigenvector exists, the nondiverging and undamped (on the fast scale) solution to Eq. (A2a′) is given by Eq. (A3a′), where a is the unknown time-dependent real amplitude. The perturbation equations of orders lower than ε^2 can be solved without requiring any solvability conditions because all of their known terms belong to the range of the operator [see Eqs. (A3b′) and (A3c′)]. However, at the ε^2 order, terms $d_1^m a\boldsymbol{u}_m$ and $d_2 d_1^{m-2} a\boldsymbol{u}_{m-1}$ appear in the equation, together with $\boldsymbol{F}_{xx}^0\boldsymbol{x}_0^2$ and $\boldsymbol{F}_{x\mu}^0\boldsymbol{x}_0\hat{\boldsymbol{\mu}}$, which are proportional to a^2 and $a\hat{\boldsymbol{\mu}}$, respectively. When solvability is enforced, a differential equation of order m is drawn, of the type given in Eq. (A4a′). When the ε^2-order equation is solved, $\boldsymbol{x}_m$ is found. It contains the term $d_2 d_1^{m-2} a\boldsymbol{u}_m$, which, at the $\varepsilon^{2+1/m}$ order, enters the solvability condition given by Eq. (A4b′) because $\boldsymbol{F}_{xx}^0\boldsymbol{x}_0\boldsymbol{x}_1$ and $\boldsymbol{F}_{x\mu}^0\boldsymbol{x}_1\hat{\boldsymbol{\mu}}$ are proportional to ad_1a and $\hat{\mu}d_1a$, respectively. By proceeding to higher orders, other solvability conditions involving combinations of derivatives, such as Eq. (A4c′) are found, that is, terms of the mth derivative of a:

$$\frac{\mathrm{d}^m a}{\mathrm{d}t^m} = \varepsilon\left[\mathrm{d}_1^m + m\varepsilon^{1/m}\,\mathrm{d}_1^{m-1}\,\mathrm{d}_2 + \varepsilon^{2/m}\left(m\,\mathrm{d}_1^{m-1}\,\mathrm{d}_3 + \frac{1}{2}m(m-1)\,\mathrm{d}_1^{m-2}\,\mathrm{d}_2^2\right) + \cdots\right]a \tag{8}$$

Therefore, by combining all of the solvability conditions in a single equation, a reconstituted bifurcation equation is obtained, given by Eq. (A5′), comprising a differential equation of the mth order, where the parameter ε has been reabsorbed according to the rules $\varepsilon a \to a$, $\varepsilon\hat{\boldsymbol{\mu}} \to \boldsymbol{\mu}$, and $\varepsilon^{1/m}\,\mathrm{d}/\mathrm{d}t \to \mathrm{d}/\mathrm{d}t$. In Eq. (A5′) $D^m a$ is a term of the ε^2 order, whereas the right-hand member contains (separated by semicolons) all of the terms of the order $\varepsilon^2, \varepsilon^{2+1/m}, \varepsilon^{2+2/m}, \ldots$, up to the highest order accounted for in the analysis. For example, if $m = 3$, the bifurcation equation at the ε^3 order reads

$$\dddot{a} = \mathscr{L}(a\boldsymbol{\mu}, a^2; \dot{a}\boldsymbol{\mu}, a\dot{a}; \ddot{a}\boldsymbol{\mu}, a\ddot{a}, \dot{a}^2; \boldsymbol{\mu}^3, a^2\boldsymbol{\mu}, a^3, \dot{a}\ddot{a}) \tag{9}$$

whereas at the $\varepsilon^{10/3}$ order, that is, one step further, it becomes

$$\dddot{a} = \mathscr{L}(\ldots; \dot{a}\boldsymbol{\mu}^2, a^2\dot{a}, a\dot{a}\boldsymbol{\mu}, \ddot{a}^2) \tag{10}$$

where only additional terms are displayed. Equation (A5′) could be referred to as a generalized Bogdanova–Arnold normal form bifurcation equation for the multiple-zero bifurcation.

III. Double-Zero Bifurcation

The multiple-scale procedure developed in the preceding section is adopted for a system that exhibits a double-zero eigenvalue ($m = 2$).

Let $(\boldsymbol{u}_1, \boldsymbol{u}_2)$ be the chain of the generalized right eigenvector and $\boldsymbol{v}_2$ the proper left eigenvector. It is further assumed that at least one of the two coefficients $\boldsymbol{v}_2^T \boldsymbol{F}^0_{x\mu}\boldsymbol{u}_1$ is different from zero, that is, the singular case discussed in Sec. II.A is excluded. This property ensures that a divergence boundary $\mathcal{D}$ and a Hopf boundary $\mathcal{H}$ originate from O, as assumed in the Takens–Bogdanova bifurcation. If this hypothesis is removed, other mechanisms leading to the double zero bifurcation can exist, namely, the double divergence, the double divergence-Hopf, and the degenerate Hopf bifurcation, not analyzed here.[11]

When $m = 2$ is assumed in the series expansion (A1′) of Appendix A, the following perturbation equations are drawn:

$$\varepsilon:\ \left(\mathrm{d}_0 - \boldsymbol{F}^0_x\right)\boldsymbol{x}_0 = 0, \qquad \varepsilon^{\frac{3}{2}}:\ \left(\mathrm{d}_0 - \boldsymbol{F}^0_x\right)\boldsymbol{x}_1 = -\mathrm{d}_1\boldsymbol{x}_0$$

$$\varepsilon^2:\ \left(\mathrm{d}_0 - \boldsymbol{F}^0_x\right)\boldsymbol{x}_2 = -\mathrm{d}_1\boldsymbol{x}_1 - \mathrm{d}_2\boldsymbol{x}_0 + \tfrac{1}{2}\boldsymbol{F}^0_{xx}\boldsymbol{x}_0^2 + \boldsymbol{F}^0_{x\mu}\boldsymbol{x}_0\hat{\boldsymbol{\mu}}$$

$$\varepsilon^{\frac{5}{2}}:\ \left(\mathrm{d}_0 - \boldsymbol{F}^0_x\right)\boldsymbol{x}_3 = -\mathrm{d}_1\boldsymbol{x}_2 - \mathrm{d}_2\boldsymbol{x}_1 - \mathrm{d}_3\boldsymbol{x}_0 + \boldsymbol{F}^0_{xx}\boldsymbol{x}_0\boldsymbol{x}_1 + \boldsymbol{F}^0_{x\mu}\boldsymbol{x}_1\hat{\boldsymbol{\mu}}$$

$$\varepsilon^3:\ \left(\mathrm{d}_0 - \boldsymbol{F}^0_x\right)\boldsymbol{x}_4 = -\mathrm{d}_1\boldsymbol{x}_3 - \mathrm{d}_2\boldsymbol{x}_2 - \mathrm{d}_3\boldsymbol{x}_1 - \mathrm{d}_4\boldsymbol{x}_0 + \boldsymbol{F}^0_{xx}\boldsymbol{x}_0\boldsymbol{x}_2 + \tfrac{1}{2}\boldsymbol{F}^0_{xx}\boldsymbol{x}_1^2 + \boldsymbol{F}^0_{x\mu}\boldsymbol{x}_2\hat{\boldsymbol{\mu}} + \tfrac{1}{6}\boldsymbol{F}^0_{xxx}\boldsymbol{x}_0^3 + \tfrac{1}{2}\boldsymbol{F}^0_{xx\mu}\boldsymbol{x}_0^2\hat{\boldsymbol{\mu}} + \tfrac{1}{2}\boldsymbol{F}^0_{x\mu\mu}\boldsymbol{x}_0\hat{\boldsymbol{\mu}}^2$$

$$\varepsilon^{\frac{7}{2}}:\ \left(\mathrm{d}_0 - \boldsymbol{F}^0_x\right)\boldsymbol{x}_5 = -\mathrm{d}_1\boldsymbol{x}_4 - \mathrm{d}_2\boldsymbol{x}_3 - \mathrm{d}_3\boldsymbol{x}_2 - \mathrm{d}_4\boldsymbol{x}_1 - \mathrm{d}_5\boldsymbol{x}_0 + \boldsymbol{F}^0_{xx}\boldsymbol{x}_0\boldsymbol{x}_3 + \boldsymbol{F}^0_{xx}\boldsymbol{x}_1\boldsymbol{x}_2 + \boldsymbol{F}^0_{x\mu}\boldsymbol{x}_3\hat{\boldsymbol{\mu}} + \tfrac{1}{2}\boldsymbol{F}^0_{xxx}\boldsymbol{x}_0^2\boldsymbol{x}_1 + \boldsymbol{F}^0_{xx\mu}\boldsymbol{x}_0\boldsymbol{x}_1\hat{\boldsymbol{\mu}} + \tfrac{1}{2}\boldsymbol{F}^0_{x\mu\mu}\boldsymbol{x}_1\hat{\boldsymbol{\mu}}^2 \tag{11}$$

Note that, if only steady-state solutions are sought, $\mathrm{d}_k \equiv 0\ \forall k$ must be posed in Eq. (11), so that $\boldsymbol{x}_k \equiv \boldsymbol{0}, k = 1, 3, \ldots$, follows. Therefore, all fractional powers of $\boldsymbol{x}$ vanish, and Eq. (11) coincides with the classical perturbation equations of the buckling analysis.[18]

When the same steps as in Appendix A are followed, solutions are found:

$$\boldsymbol{x}_0 = a\boldsymbol{u}_1, \qquad \boldsymbol{x}_1 = \mathrm{d}_1 a\boldsymbol{u}_2, \qquad \boldsymbol{x}_2 = \mathrm{d}_2 a\boldsymbol{u}_2 + \tfrac{1}{2}a^2\boldsymbol{z}_2 + a\boldsymbol{Z}_2\hat{\boldsymbol{\mu}}$$

$$\boldsymbol{x}_3 = \mathrm{d}_3 a\boldsymbol{u}_2 + a\,\mathrm{d}_1 a\boldsymbol{z}_{\frac{5}{2}} + \mathrm{d}_1 a\boldsymbol{Z}_{\frac{5}{2}}\hat{\boldsymbol{\mu}}$$

$$\boldsymbol{x}_4 = (\mathrm{d}_1 a)^2\boldsymbol{z}_{31} + \mathrm{d}_1^2 a(a\boldsymbol{z}_{32} + \boldsymbol{Z}_{31}\hat{\boldsymbol{\mu}}) + \mathrm{d}_2 a\left(a\boldsymbol{z}_{\frac{5}{2}} + \boldsymbol{Z}_{\frac{5}{2}}\hat{\boldsymbol{\mu}}\right) + a^3\boldsymbol{z}_{33} + a^2\boldsymbol{Z}_{32}\hat{\boldsymbol{\mu}} + a\boldsymbol{Z}_{33}\hat{\boldsymbol{\mu}}^2 \tag{12}$$

where $\boldsymbol{z}_2 \in \Re^n$ and $\boldsymbol{Z}_2 \in \Re^n \times \Re^2, \ldots$ are solutions of linear algebraic equations reported in Appendix B.

Similarly, the following solvability conditions are found at the various orders:

$$\varepsilon^2:\ \mathrm{d}_1^2 a = a\boldsymbol{k}_1\hat{\boldsymbol{\mu}} + \tfrac{1}{2}a^2 k_2, \qquad \varepsilon^{\frac{5}{2}}:\ 2\,\mathrm{d}_1\,\mathrm{d}_2 a = \mathrm{d}_1 a(\boldsymbol{k}_3\hat{\boldsymbol{\mu}} + k_4 a)$$

$$\varepsilon^3:\ 2\,\mathrm{d}_1\,\mathrm{d}_3 a + \mathrm{d}_2^2 a = \mathrm{d}_2 a(\boldsymbol{k}_3\hat{\boldsymbol{\mu}} + k_4 a) + k_5(\mathrm{d}_1 a)^2 + k_6 a^3 + \boldsymbol{k}_7\hat{\boldsymbol{\mu}}a^2 + \boldsymbol{k}_8\hat{\boldsymbol{\mu}}^2 a + \mathrm{d}_1^2 a(h_1 a + \boldsymbol{h}_2\hat{\boldsymbol{\mu}})$$

$$\varepsilon^{\frac{7}{2}}:\ 2\,\mathrm{d}_2\,\mathrm{d}_3 a + 2\,\mathrm{d}_1\,\mathrm{d}_4 a = \mathrm{d}_3 a(\boldsymbol{k}_3\hat{\boldsymbol{\mu}} + k_4 a) + k_5(2\,\mathrm{d}_1 a\,\mathrm{d}_2 a)^2 + \mathrm{d}_1 a\left[k_9 a^2 + \boldsymbol{k}_{10}\hat{\boldsymbol{\mu}}a + \boldsymbol{k}_{11}\hat{\boldsymbol{\mu}}^2 + (h_3 + h_4)\,\mathrm{d}_1^2 a\right] + \mathrm{d}_1\left(\mathrm{d}_1^2 a\right)(h_4 a + \boldsymbol{h}_5\hat{\boldsymbol{\mu}}) + 2\,\mathrm{d}_1\,\mathrm{d}_2 a(h_6 a + \boldsymbol{h}_7\hat{\boldsymbol{\mu}}) \tag{13}$$

where the coefficients $\boldsymbol{k}_i$ and $\boldsymbol{h}_i$ are defined in Appendix C. Equations (13), after using Eq. (8) (with $m = 2$), lead to

$$\ddot{a} = \left(-\boldsymbol{k}_1\boldsymbol{\mu} + \boldsymbol{k}_8\boldsymbol{\mu}^2\right)a + \left(-\boldsymbol{k}_3\boldsymbol{\mu} + \boldsymbol{k}_{11}\boldsymbol{\mu}^2\right)\dot{a} + (k_2 + \boldsymbol{k}_7\boldsymbol{\mu})a^2 + (k_4 + \boldsymbol{k}_{10}\boldsymbol{\mu})a\dot{a} + k_5\dot{a}^2 + k_6 a^3 + k_9 a^2\dot{a} \tag{14}$$

in which the coefficient $\boldsymbol{k}_1\boldsymbol{\mu}$ is not identically zero, by virtue of the hypothesis assumed. In Eq. (4), the parameter ε has been reabsorbed in accordance with the position $\boldsymbol{\mu} = \varepsilon\hat{\boldsymbol{\mu}}$ and the rules $\varepsilon a \to a$, $\varepsilon^{1/2}\,\mathrm{d}/\mathrm{d}t \to \mathrm{d}/\mathrm{d}t$. Equation (14) is Bogdanova–Arnold's, improved up to the order $\varepsilon^{7/2}$. It is the equation of motion of a nonlinear single-degree-of-freedom system with quadratic and cubic nonlinearities.

IV. Steady-State Solutions and Stability

From the bifurcation equation (14), steady solutions $a = a_s =$ const are drawn, and their stability investigated through a straightforward perturbation analysis, as will be described.

The linear parts of the coefficients of a and $\dot{a}$ in Eq. (14), namely, $\kappa := \boldsymbol{k}_1\boldsymbol{\mu}$ and $\xi := \boldsymbol{k}_3\boldsymbol{\mu}$, are taken as unfolding parameters and are assumed to be of order ε. By the vanishing of time derivatives ($\dot{a}_s = \ddot{a}_s = 0$) and the expanding of a_s as $a_s = \varepsilon a_1 + \varepsilon^2 a_2 + \cdots$, perturbation equations of the following type are drawn at the leading orders:

$$\varepsilon^2:\ (\kappa + k_2 a_1)a_1 = 0 \tag{15a}$$

$$\varepsilon^3:\ (\kappa + k_2 a_1)a_2 = h(a_1, \kappa, \xi) \tag{15b}$$

From Eq. (15a) both trivial (T) and nontrivial (NT) solutions are found, depending only on κ; from Eq. (15b), higher-order corrections to the NT solution are drawn, also depending on ξ.

The stability of both the T solution and the NT solution is analyzed by taking the variation of the bifurcation equation (14). This leads to a second-degree algebraic equation in the eigenvalue σ, which governs the evolution of the perturbation,

$$\sigma^2 + I_1\sigma + I_2 = 0 \tag{16}$$

where $I_k = I_k[a_s(\kappa, \xi), \kappa, \xi]$ are the invariants of the variational matrix. It is well known that this equation admits the following critical boundaries on the invariant (I_1, I_2) plane: a divergence locus $\mathcal{D}$, of equation $I_2 = 0$; a Hopf locus $\mathcal{H}$, of equation $I_1 = 0$; and a nilpotent locus $\mathcal{N}$, of equation $I_1^2 - 4I_2 = 0$. To map the loci on the unfolding (κ, ξ) plane, the parameters are expanded as $\kappa = \varepsilon\kappa_1 + \varepsilon^2\kappa_2 + \cdots$ and $\xi = \varepsilon\xi_1 + \varepsilon^2\xi_2 + \cdots$ and substituted in the loci equations. When terms with the same power of ε are zeroed, ε^2- and ε^3-order perturbation equations are drawn. From the first set of equations, relationships of the type $f(\kappa_1, \xi_1) = 0$ are obtained, which describe the critical boundaries at the first order. From the second set of equations, relationships of the type $g(\kappa_2, \xi_2, \kappa_1^2, \xi_1^2, \kappa_1\xi_1) = 0$ are derived. When these are recombined according to $\varepsilon^2 f(\cdot) + \varepsilon^3 g(\cdot) = 0$, and the parameters are reconstituted, a second-order approximation of the boundaries is finally obtained. The results are illustrated in detail in Appendix D.

V. Numerical Evaluation of the Bifurcation Equation Coefficients

To show the effectiveness of the proposed method, an algorithm is described for numerically evaluating the coefficients of the bifurcation equation (14) for a class of systems. The method does not require the repetition of the whole procedure for the specific system at hand, but only evaluation of the numerical coefficients by performing elementary operations. In this respect the method is user oriented, different from other methods, such as the center manifold method, which have not yet been implemented to furnish ready-to-use formulas.

A broad class of N-dimensional mechanical systems is considered, having equations

$$\dot{\boldsymbol{x}} = (\boldsymbol{A} + \boldsymbol{\mu}\boldsymbol{B})\boldsymbol{x} + \boldsymbol{c}(\boldsymbol{x}) \tag{17}$$

where the matrices $\boldsymbol{A}$ and $\boldsymbol{B}$ are constant and the vector $\boldsymbol{c}(\boldsymbol{x})$ collects quadratic and cubic nonlinearities independent of $\boldsymbol{\mu}$. Therefore, the ith equation (17) is

$$\dot{x}_i = \sum_i a_{ij}x_j + \sum_{j,k}\mu_j b_{ijk}x_k + \frac{1}{2}\sum_{j,k} c_{ijk}x_j x_k + \frac{1}{6}\sum_{j,k,l} c_{ijkl}x_j x_k x_l \tag{18}$$

where coefficients c are symmetrical with respect to indices j, k, and l. For this class, $\boldsymbol{F}_x^0 = \boldsymbol{A}$, $F_{xx\mu}^0 = 0$, and $\boldsymbol{F}_{x\mu\mu}^0 = \boldsymbol{0}$. The following functions are defined:

$$f(\boldsymbol{v}, \boldsymbol{u}, \boldsymbol{\mu}) := \boldsymbol{v}^T\boldsymbol{F}_{x\mu}^0\boldsymbol{u}\boldsymbol{\mu} = \sum_{i,j,k} b_{ijk}v_i u_j \mu_k$$

$$g(\boldsymbol{v}, \boldsymbol{u}, \boldsymbol{w}) := \boldsymbol{v}^T\boldsymbol{F}_{xx}^0\boldsymbol{u}\boldsymbol{w} = \sum_{i,j,k} c_{ijk}v_i u_j w_k$$

$$h(\boldsymbol{v}, \boldsymbol{u}, \boldsymbol{w}, \boldsymbol{y}) := \boldsymbol{v}^T\boldsymbol{F}_{xxx}^0\boldsymbol{u}\boldsymbol{w}\boldsymbol{y} = \sum_{i,j,k,l} c_{ijkl}v_i u_j w_k y_l \tag{19}$$

The preceding functions associate a real number with the dummy vectors $\boldsymbol{v}$, $\boldsymbol{u}$, $\boldsymbol{\mu}$, $\boldsymbol{w}$, and $\boldsymbol{y}$. When the arguments are chosen appropriately, the functions (19) furnish all of the quantities necessary to evaluate the coefficients appearing in the bifurcation equation (14). In particular, by taking $\boldsymbol{v}$ equal to the canonical vector $\boldsymbol{e}_j = \{\delta_{ij}\}$, $j = 1, 2, \ldots, N$, they also make it possible to build up the vector equations in Appendix B.

The following step-by-step algorithm is applied:

1) Proper and generalized right eigenvectors are evaluated at the bifurcation point $\boldsymbol{\mu} = \boldsymbol{0}$ by solving the equations $\boldsymbol{A}\boldsymbol{u}_1 = \boldsymbol{0}$, $\boldsymbol{A}\boldsymbol{u}_2 = \boldsymbol{u}_1$, $\boldsymbol{A}^T\boldsymbol{v}_2 = \boldsymbol{0}$, and $\boldsymbol{A}^T\boldsymbol{v}_1 = \boldsymbol{v}_2$ and normalizing the solutions according to $\boldsymbol{v}_j^T\boldsymbol{u}_k = \delta_{jk}$.

2) The known terms of Eqs. (B1a) are built up as

$$\boldsymbol{F}_{xx}^0\boldsymbol{u}_1^2 = \{g(\boldsymbol{e}_j, \boldsymbol{u}_1, \boldsymbol{u}_1)\}, \qquad \left(\boldsymbol{v}_2^T\boldsymbol{F}_{xx}^0\boldsymbol{u}_1^2\right)\boldsymbol{u}_2 = \{g(\boldsymbol{v}_2, \boldsymbol{u}_1, \boldsymbol{u}_1)\boldsymbol{u}_2\} \tag{20}$$

where braces collect the vector coefficients for j running from 1 to N. Then z_2 is evaluated by solving the singular equation (B1a) under the constraint condition $\boldsymbol{v}_1^T z_2 = 0$.

3) To solve Eq. (B1b), $\boldsymbol{\mu}$ is first set equal to the canonical vector $\boldsymbol{e}_k$. The known terms then are

$$\boldsymbol{F}_{x\mu}^0\boldsymbol{u}_1\boldsymbol{e}_k = \{f(\boldsymbol{e}_j, \boldsymbol{u}_1, \boldsymbol{e}_k)\}$$

$$\left(\boldsymbol{v}_2^T\boldsymbol{F}_{x\mu}^0\boldsymbol{u}_1\boldsymbol{e}_k\right)\boldsymbol{u}_2 = \{f(\boldsymbol{v}_2, \boldsymbol{u}_1, \boldsymbol{e}_k)\boldsymbol{u}_2\} \tag{21}$$

When the relevant equation is solved, the kth column of the matrix $\boldsymbol{Z}_2$ is evaluated, provided it is orthogonal to $\boldsymbol{v}_1$. When k is allowed to run from 1 to m, the whole matrix $\boldsymbol{Z}_2$ is obtained.

4) When arguments similar to steps 2 and 3 are used, all Eqs. (B2) and (B3) are solved and $(z_{5/2}, z_{31}, z_{32}, z_{33})$ as well as $(\boldsymbol{Z}_{5/2}, \boldsymbol{Z}_{31}, \boldsymbol{Z}_{32}, \boldsymbol{Z}_{33})$ are sequentially evaluated.

5) Constants h_1, h_3, h_4, h_6, and h_8 and vectors $\boldsymbol{h}_2$ and $\boldsymbol{h}_5$ in Eqs. (C1) are straigthforwardly calculated; vectors $\boldsymbol{h}_7$ and $\boldsymbol{h}_9$ instead call for use of the functions (19) with canonical vectors, for example,

$$\boldsymbol{h}_7 = \{f(\boldsymbol{v}_2, \boldsymbol{u}_1, \boldsymbol{e}_k)\} \tag{22}$$

6) Coefficients $\boldsymbol{k}$ in Eqs. (14) are finally evaluated by Eqs. (C2), for example,

$$\boldsymbol{k}_3 = \left\{-f(\boldsymbol{v}_2, \boldsymbol{u}_2, \boldsymbol{e}_k) + \boldsymbol{v}_2^T\boldsymbol{Z}_2\boldsymbol{e}_k\right\} \tag{23}$$

7) After the bifurcation equation (14) has been numerically integrated for a given set of parameters and given initial conditions, and the amplitude $a(t)$ and its derivatives have been evaluated, the state $\boldsymbol{x}(t)$ is obtained by Eqs. (A1a′) in Appendix A and Eqs. (12), where all of the quantities are now known.

Note that the described procedure makes it possible to obtain a bifurcation equation that is parametric in $\boldsymbol{\mu}$, so that the procedure does not have to be repeated for any choice of $\boldsymbol{\mu}$. Once the algorithm has been implemented, only the coefficients a_{ij}, b_{ijk}, c_{ijk}, and c_{ijkl} in Eqs. (19) must be given for any specific system.

VI. Sample Mechanical System

In this section, the structure shown in Fig. 1 is studied. It consists of a double pendulum with two concentrated masses m_1 and m_2 loaded by a follower force F applied at the end. The rods are rigid and massless; the elastic springs are nonlinear and produce restoring forces $f_i = f_i(e_i)$, $i = 1, 2$, where e_i are the strains. Finally, the viscous devices are linear, of coefficients c_i. If the constitutive nonlinearities of the springs are neglected, the structure reduces to that studied in Ref. 19. When rotations q_i, $i = 1, 2$, in Fig. 1 are assumed as Lagrangian parameters, the dimensional nonlinear equations of motion are

$$\begin{aligned}
&(m_1 + m_2)l^2\ddot{q}_1 + m_2 l^2\left[\cos(q_1 - q_2)\ddot{q}_2 - \sin(q_2 - q_1)\dot{q}_2^2\right] \\
&\quad + \left(c_1 + c_2 + 2c_3 l^2\cos^2 q_1\right)\dot{q}_1 + \left(c_3 l^2\cos q_1\cos q_2 - c_2\right)\dot{q}_2 \\
&\quad + f_1(e_1) - f_2(e_2) + f_3(e_3)l\cos q_1 + Fl\sin(q_2 - q_1) = 0 \\
&m_2 l^2\ddot{q}_2 + m_2 l^2\left[\cos(q_1 - q_2)\ddot{q}_1 - \sin(q_1 - q_2)\dot{q}_1^2\right] \\
&\quad + \left(c_2 + c_3 l^2\cos^2 q_2\right)\dot{q}_2 + \left(c_3 l^2\cos q_1\cos q_2 - c_2\right)\dot{q}_1 \\
&\quad + f_2(e_2) + f_3(e_3)l^2\cos q_2 = 0
\end{aligned} \tag{24}$$

where $e_1 = q_1$, $e_2 = q_2 - q_1$, and $e_3 = l(\sin q_1 + \sin q_2)$. It is assumed, for simplicity, that $f_2 = f_1$, $c_2 = c_1$, $m_1 = 2m$, and $m_2 = m$. When Eqs. (24) are expanded in Mac Laurin series up to cubic terms, and the following nondimensional quantities are taken into account:

$$\hat{\alpha} = k_3^{(1)}\big/m\omega^2, \qquad a_2 = k_3^{(2)}l\big/m\omega^2, \qquad a_3 = k_3^{(3)}l^2\big/m\omega^2$$

$$b_1 = k_1^{(1)}\big/ml^2\omega^2, \qquad b_2 = k_1^{(2)}\big/ml^2\omega^2, \qquad b_3 = k_1^{(3)}\big/ml^2\omega^2$$

$$\hat{\beta} = F\big/ml\omega^2, \qquad c = c_1\big/ml^2\omega, \qquad d = (c_3/c_1)l^2 \tag{25}$$

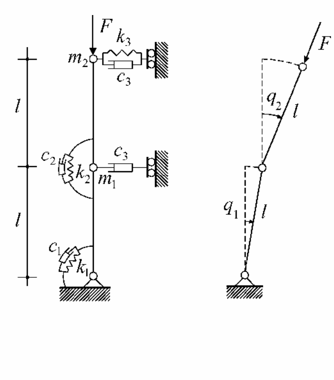

Fig. 1 Double pendulum loaded by a follower force *F*.

the nondimensional equation of motion are put in the form given by Eqs. (17) and (18), where now $\boldsymbol{x} = (x_1, x_2, x_3, x_4)^T = (q_1, \dot{q}_1, q_2, \dot{q}_2)^T$ and $\boldsymbol{c}(\boldsymbol{x}) = [0, c_1(\boldsymbol{x}), 0, c_2(\boldsymbol{x})]^T$. In Eqs. (25), $k_i^{(1)}$ is the linear stiffness of the springs, and $k_i^{(2)}$ and $k_i^{(3)}$ are the quadratic and cubic stiffnesses, that is, $f_i = k_i^{(1)} e_i + k_i^{(2)} e_i^2/2 + k_i^{(3)} e_i^3/6$. Moreover, ω is a scaling factor having the dimension of a frequency, and $\tau = \omega t$ is a nondimensional time. The parameters $(\hat{\alpha}, \hat{\beta})$ are assumed as control parameters, representing the nondimensional stiffness of the extensional spring and the load, respectively. In addition $(\alpha, \beta) = \boldsymbol{\mu}$ are their increments from the bifurcation values $(\alpha_0, \beta_0) = (0.150, 5.827)$, where the system exibits a double-zero eigenvalue, that is, $(\alpha, \beta) = (\hat{\alpha}, \hat{\beta}) - (\alpha_0, \beta_0)$ (Fig. 2). The values of the remaining auxiliary parameters are fixed at $b_1 = 1$, $c = 1.5$, and $d = 0.5$, that is, the same values assumed in Ref. 19. In addition, $a_2 = 1$, $a_3 = 1$, $b_2 = 1$, and $b_3 = 1$ are taken. Numerical values of nonvanishing coefficients in the equations of motion (18) are $a_{12} = 1$, $a_{21} = 1.41$, $a_{22} = -2.63$, $a_{23} = -1.91$, $a_{24} = 1.5$, $a_{34} = 1$, $a_{41} = -0.56$, $a_{42} = 3.37$, $a_{43} = 0.76$, $a_{44} = -3.75$; $b_{221} = 0.5$, $b_{411} = -0.5$, $b_{421} = -0.5$, $b_{413} = -1$, $b_{423} = 0.5$; $c_{211} = 0.25$, $c_{213} = -1$, $c_{233} = 0.5$, $c_{411} = -1.25$, $c_{413} = 1$, $c_{433} = -1.5$, $c_{2111} = 0.75$, $c_{2112} = 1.88$, $c_{2122} = -0.5$, $c_{2113} = -2.25$, $c_{2123} = -3$, $c_{2223} = 0.5$, $c_{2133} = 2$, $c_{2233} = 1.31$, $c_{2333} = -0.58$, $c_{2114} = -1.13$, $c_{2134} = 2.63$, $c_{2334} = -2.25$, $c_{2144} = -0.5$, $c_{2344} = 0.5$, $c_{4111} = -1.5$, $c_{4112} = -3$, $c_{4122} = 1.5$, $c_{4113} = 3.25$, $c_{4123} = 5.63$, $c_{4223} = -1.5$, $c_{4133} = -3.75$, $c_{4233} = -2.25$, $c_{4333} = 0.75$, $c_{4114} = 1.88$, $c_{4134} = -4.13$, $c_{4334} = 3$, $c_{4144} = 0.5$, and $c_{4344} = -0.5$.

Proper and generalized eigenvectors assume the values in Table 1.

When the algorithm developed in Sec. V is applied, the following bifurcation equation is obtained:

$$\begin{aligned}\ddot{a} = {} & (1.277\alpha + 0.058\beta + 13.601\alpha^2 + 1.002\alpha\beta + 0.0002\beta^2)a \\ & + (-4.709\alpha + 0.147\beta - 81.129\alpha^2 - 0.870\alpha\beta - 0.003\beta^2)\dot{a} \\ & + (27.700\alpha + 1.131\beta + 0.837)a^2 - (444.871\alpha + 11.480\beta \\ & + 6.445)a\dot{a} + 19.912\dot{a}^2 + 12.733a^3 - 300.393a^2\dot{a} \qquad (26)\end{aligned}$$

where $\kappa := -(1.277\alpha + 0.058\beta)$ and $\xi := -(-4.709\alpha + 0.147\beta)$ are unfolding parameters, whose geometric meaning is shown in Fig. 2. The straight lines $\kappa = 0$ and $\xi = 0$ represent, on the (α, β)

Table 1 Proper and generalized eigenvectors of the sample system

$\boldsymbol{u}_1$	$\boldsymbol{u}_2$	$\boldsymbol{v}_1$	$\boldsymbol{v}_2$
0.804	1	1	2.126
0	0.804	1.947	−0.364
0.594	0.101	0.329	−2.878
0	0.594	1.110	−0.913

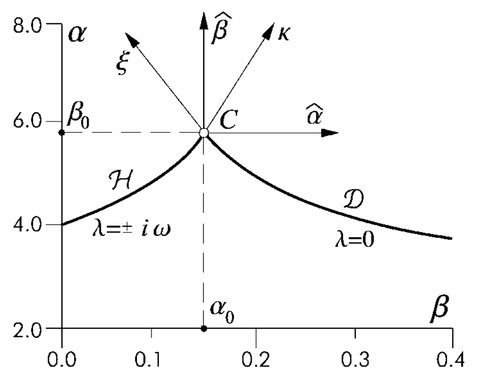

Fig. 2 Linear stability diagram.

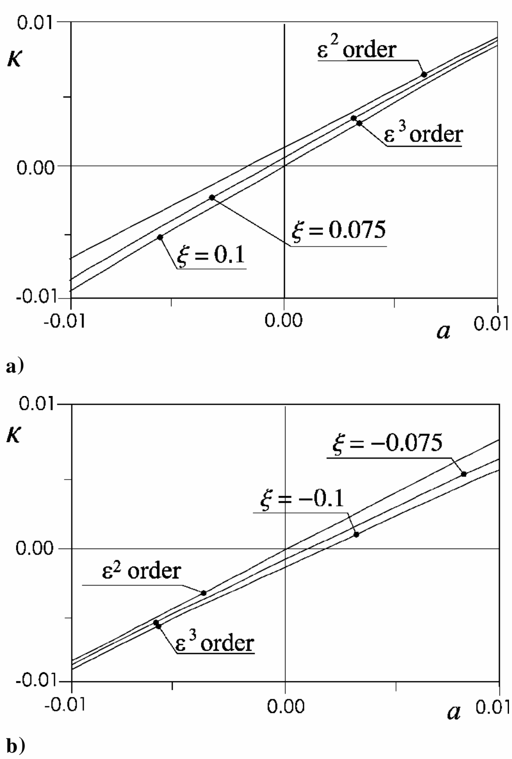

Fig. 3 Nontrivial bifurcated steady-state solution.

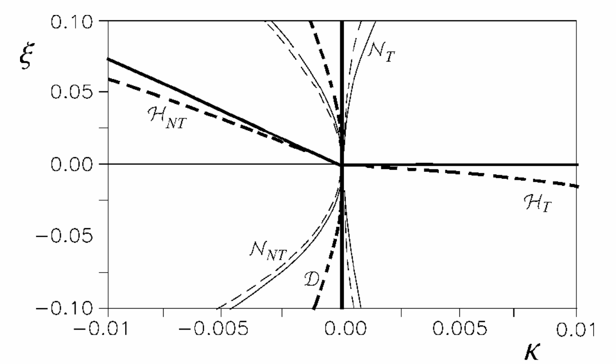

Fig. 4 Comparison among different approximations of the critical boundaries: ——, ε^2 order and - - -, ε^3 order.

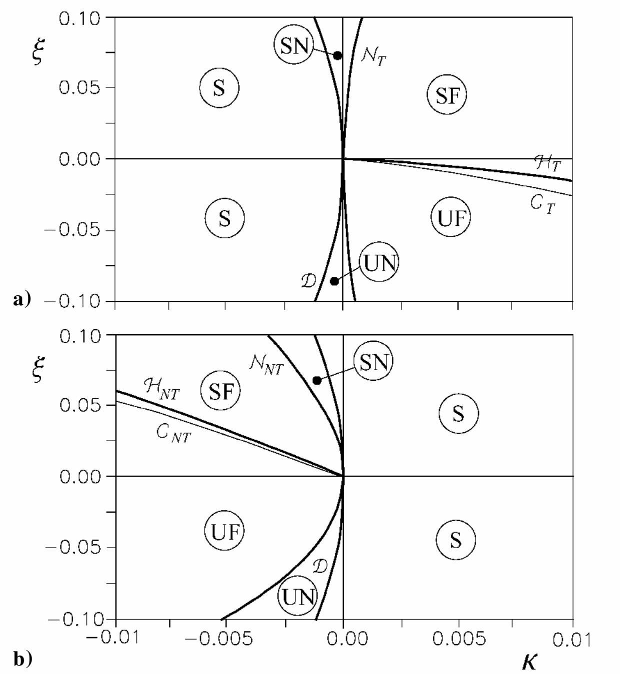

Fig. 5 Critical boundaries and quality of the motion (S, saddle; SN, stable node; SF, stable focus; UN: unstable node; and UF, unstable focus): a) trivial steady-state solution and b) nontrivial steady-state solution.

plane, the first-order approximations of the divergence $\mathcal{D}$ and Hopf $\mathcal{H}$ boundaries, respectively.

When the results of Sec. IV are used, the NT steady solutions at the ε^2 or ε^3 order are obtained; they are represented in Fig. 3 on the (a, κ) plane for positive (Fig. 3a) and negative (Fig. 3b) values of ξ. It is seen that the amplitude mainly depends on κ; it is independent of ξ at the ε^2-order, whereas it is weakly dependent on it at the ε^3 order. Accordingly, the bifurcation point depends on ξ.

Figure 4 shows a comparison among different order approximations of the critical boundaries. In Fig. 4, continuous lines represent the first approximation (ε^2 order) of the divergence $\mathcal{D}$ and Hopf $\mathcal{H}$ boundaries (coincident with the unfolding parameter axes) whereas dashed lines describe an improved (ε^3-order) approximation of the boundaries for both T and NT stationary solutions. Moreover, the $\mathcal{N}$-labeled curves represent a manifold of nilpotent systems to which the critical system belongs, that is, the locus of systems having two coincident eigenvalues.[11] In Fig. 5, the quality of motion in different regions bounded by the critical boundaries is shown, for T (Fig. 5a) and NT (Fig. 5b) stationary solutions. The $\mathcal{C}$-labeled curves represent the locus in which a homoclinic bifurcation occurs and the periodic solution collides with a saddle. They have been obtained numerically by varying the parameter κ and determining the corresponding value of the parameter ξ for which the limit cycle disappears.

To sum up, the T solution loses stability along the Hopf boundary $\mathcal{H}_T$, where a Hopf bifurcation manifests itself, and along the divergence boundary $\mathcal{D}$, where a transcritical bifurcation takes place, from which a NT solution emerges. This loses stability at the boundary $\mathcal{H}_{\mathrm{NT}}$, where a new Hopf bifurcation manifests itself. Moreover, the two further curves $\mathcal{N}_T$ and $\mathcal{N}_{\mathrm{NT}}$ organize the parameter plane, being the loci of systems having two coincident eigenvalues. Finally, along the two homoclinic boundaries $\mathcal{C}_T$ and $\mathcal{C}_{\mathrm{NT}}$, a collision between a limit cycle and a saddle point occurs. The scenario is better represented in Fig. 6, where the phase portraits of each region of the parameter plane are shown. From regions 1 to 5 or, similarly, from regions 6 to 10, the equilibrium points (E_0 and E_1, respectively, T and NT solutions) are first a stable node and a saddle; the node then modifies to become a focus; after a Hopf bifurcation, the focus becomes unstable and a limit cycle p arises; after colliding with the saddle, the limit cycle disappears; finally, the focus becomes an unstable node. Thus, in regions 1–3 and 6–8, there exists an attractor: mainly an equilibrium point because a periodic motion only occurs in a narrow region. In contrast, no attractors exist in regions 4, 5, 9, and 10.

Figure 7 shows the bifurcation diagrams along the paths represented in Fig. 6. Along path 1 (Fig. 7a), stable limit cycles are born at point A (intersection with the Hopf boundary $\mathcal{H}_T$ from the T solution, which loses stability. The boundaries of the gray region represent the maximun and minimum values of the amplitude a assumed in the periodic motion. At point B, a homoclinic bifurcation occurs, and the stable limit cycles disappear. The NT solution is always unstable. Along path 2 (Fig. 7b), stable limit cycles are born at point C (intersection with the Hopf boundary $\mathcal{H}_{\mathrm{NT}}$) from the NT solution branch, but disappear at D due to a homoclinic bifurcation; the T solution is always unstable. Along path 3 (Fig. 7c), a NT solution branch bifurcates at point E (intersection with the divergence

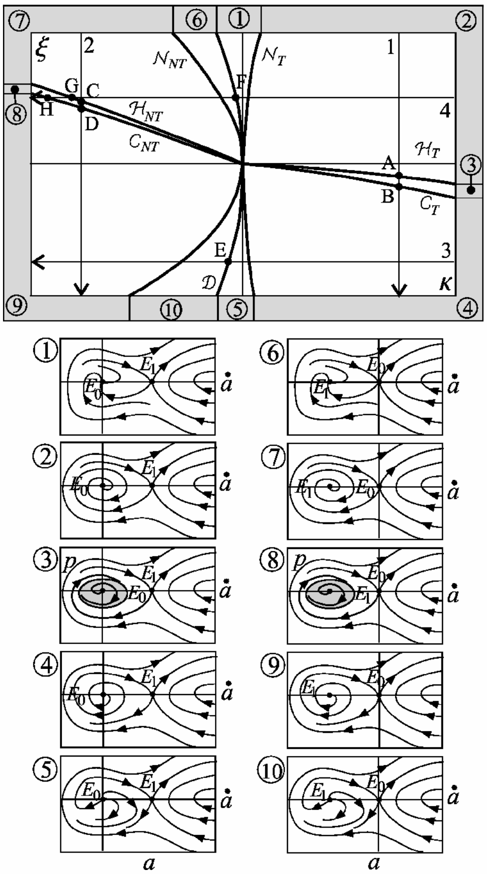

Fig. 6 Phase portraits in the (κ, ξ)-parameter plane.

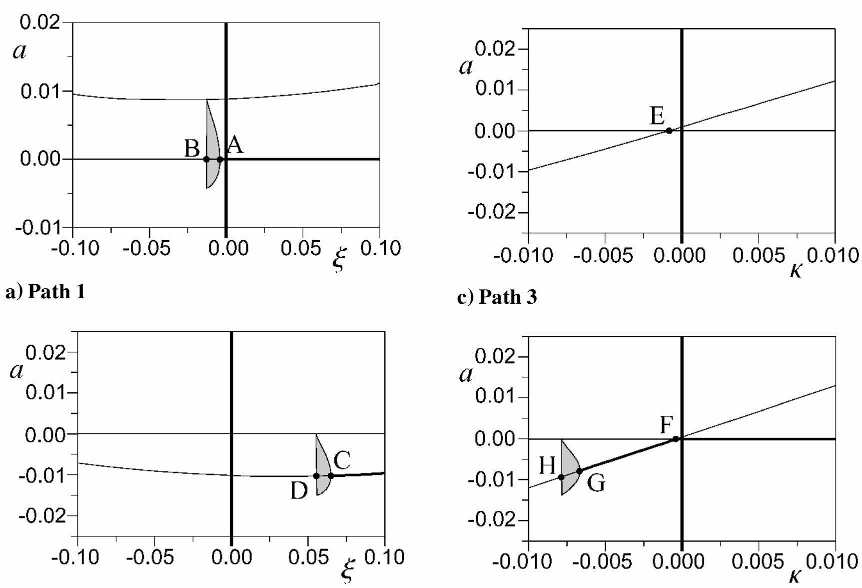

a) Path 1

b) Path 2

c) Path 3

d) Path 4

Fig. 7 Bifurcation diagrams along the path shown in Fig. 6: ▬▬, stable and ——, unstable.

boundaries $\mathcal{D}$) from the T solution. Both the T and NT solutions are always unstable. Finally, along path 4 (Fig. 7d), a stable NT solution branch bifurcates at point F (intersection with the divergence boundary $\mathcal{D}$ from the T solution, whereas stable limit cycles are born at point G (intersection with the Hopf boundary $\mathcal{H}_{NT}$) from the NT solution branch; at point H, the limit cycles disappear due to a homoclinic bifurcation.

VII. Conclusions

When the analogies between sensitivity and bifurcation analysis in defective systems are exploited, a multiple-scale algorithm is developed to obtain the bifurcation equation governing the dynamics around an m-zero eigenvalue. The method differs from other procedures applied in the analysis of both codimension-1 and -2 bifurcation problems, in that it uses suitable fractional powers of ε. When the reconstitution procedure is used, an mth-order ordinary differential equation in the unique unknown amplitude is obtained, which asymptotically governs the dynamics around the bifurcation. It generalizes the Bogdanova–Arnold normal form equation. When these results are used, the nonlinear behavior of general dynamic systems in the control parameter space around a double-zero eigenvalue is analyzed. Finally, a mechanical system is considered, and the theory is applied to describe the nonlinear behavior around the bifurcation.

Appendix A: Eigenpair Sensitivity and Bifurcation Analysis for a Defective Multiple-Zero Eigenvalue

Sensitivity Analysis

$$\boldsymbol{w} = \boldsymbol{w}_0 + \varepsilon^{1/m}\boldsymbol{w}_1 + \varepsilon^{2/m}\boldsymbol{w}_2 + \cdots \tag{A1a}$$

$$\lambda = \lambda_0 + \varepsilon^{1/m}\lambda_1 + \varepsilon^{2/m}\lambda_2 + \cdots \tag{A1b}$$

$$\varepsilon^0 : (\boldsymbol{A}_0 - \lambda_0\boldsymbol{I})\boldsymbol{w}_0 = \boldsymbol{0} \tag{A2a}$$

$$\varepsilon^{1/m} : (\boldsymbol{A}_0 - \lambda_0\boldsymbol{I})\boldsymbol{w}_1 = \lambda_1\boldsymbol{w}_0 \tag{A2b}$$

$$\varepsilon^{2/m} : (\boldsymbol{A}_0 - \lambda_0\boldsymbol{I})\boldsymbol{w}_2 = \lambda_1\boldsymbol{w}_1 + \lambda_2\boldsymbol{w}_0 \tag{A2c}$$

$$\cdots\cdots\cdots\cdots\cdots\cdots\cdots\cdots$$

$$\varepsilon : (\boldsymbol{A}_0 - \lambda_0\boldsymbol{I})\boldsymbol{w}_m = \lambda_1\boldsymbol{w}_{m-1} + \lambda_2\boldsymbol{w}_{m-2} + \cdots - \boldsymbol{A}_1\boldsymbol{w}_0 \tag{A2d}$$

$$\varepsilon^{1+1/m} : (\boldsymbol{A}_0 - \lambda_0\boldsymbol{I})\boldsymbol{w}_{m+1} = \lambda_1\boldsymbol{w}_m + \lambda_2\boldsymbol{w}_{m-1} + \cdots \tag{A2e}$$

$$\varepsilon^0 : \boldsymbol{w}_0 = \boldsymbol{u}_1 \tag{A3a}$$

$$\varepsilon^{1/m} : \boldsymbol{w}_1 = \lambda_1\boldsymbol{u}_2 \tag{A3b}$$

$$\varepsilon^{2/m} : \boldsymbol{w}_2 = \lambda_1^2\boldsymbol{u}_3 + \lambda_2\boldsymbol{u}_2 \tag{A3c}$$

$$\cdots\cdots\cdots\cdots\cdots\cdots\cdots\cdots$$

$$\lambda_1^m = \boldsymbol{v}_m^H\boldsymbol{A}_1\boldsymbol{u}_1 \tag{A4a}$$

$$m\lambda_2\lambda_1^{m-1} = f(\lambda_1) \tag{A4b}$$

$$m\lambda_3\lambda_1^{m-1} = f(\lambda_1, \lambda_2) \tag{A4c}$$

$$\lambda^m + c_1(\boldsymbol{\mu})\lambda^{m-1} + \cdots + c_m(\boldsymbol{\mu}) = 0 \tag{A5}$$

Bifurcation Analysis

$$\boldsymbol{x} = \varepsilon(\boldsymbol{x}_0 + \varepsilon^{1/m}\boldsymbol{x}_1 + \varepsilon^{2/m}\boldsymbol{x}_2 + \cdots) \tag{A1a$'$}$$

$$\frac{\mathrm{d}}{\mathrm{d}t} = \mathrm{d}_0 + \varepsilon^{1/m}\,\mathrm{d}_1 + \varepsilon^{2/m}\,\mathrm{d}_2 + \cdots \tag{A1b$'$}$$

$$\varepsilon : \left(\mathrm{d}_0 - \boldsymbol{F}_x^0\right)\boldsymbol{x}_0 = 0 \tag{A2a$'$}$$

$$\varepsilon^{1+1/m} : \left(\mathrm{d}_0 - \boldsymbol{F}_x^0\right)\boldsymbol{x}_1 = -\mathrm{d}_1\boldsymbol{x}_0 \tag{A2b$'$}$$

$$\varepsilon^{1+2/m} : \left(\mathrm{d}_0 - \boldsymbol{F}_x^0\right)\boldsymbol{x}_2 = -\mathrm{d}_1x_1 - \mathrm{d}_2\boldsymbol{x}_0 \tag{A2c$'$}$$

$$\cdots\cdots\cdots\cdots\cdots\cdots\cdots\cdots$$

$$\begin{aligned}\varepsilon^2 : \left(\mathrm{d}_0 - \boldsymbol{F}_x^0\right)\boldsymbol{x}_m &= -\mathrm{d}_1\boldsymbol{x}_{m-1} - \mathrm{d}_2\boldsymbol{x}_{m-2}\\ &\quad + \cdots + \frac{1}{2}\boldsymbol{F}_{xx}^0\boldsymbol{x}_0^2 + \boldsymbol{F}_{x\mu}^0\boldsymbol{x}_0\hat{\boldsymbol{\mu}}\end{aligned} \tag{A2d$'$}$$

$$\begin{aligned}\varepsilon^{2+1/m} : \left(\mathrm{d}_0 - \boldsymbol{F}_x^0\right)\boldsymbol{x}_{m+1} &= -\mathrm{d}_1\boldsymbol{x}_m - \mathrm{d}_2\boldsymbol{x}_{m-1}\\ &\quad + \cdots + \boldsymbol{F}_{xx}^0\boldsymbol{x}_0\boldsymbol{x}_1 + \boldsymbol{F}_{x\mu}^0\boldsymbol{x}_1\hat{\boldsymbol{\mu}}\end{aligned} \tag{A2e$'$}$$

$$\varepsilon : \boldsymbol{x}_0 = a(t_1, t_2, \ldots)\boldsymbol{u}_1 \tag{A3a$'$}$$

$$\varepsilon^{1+1/m} : \boldsymbol{x}_1 = \mathrm{d}_1a\boldsymbol{u}_2 \tag{A3b$'$}$$

$$\varepsilon^{1+2/m} : \boldsymbol{x}_2 = \mathrm{d}_1^2a\boldsymbol{u}_3 + \mathrm{d}_2a\boldsymbol{u}_2 \tag{A3c$'$}$$

$$\cdots\cdots\cdots\cdots\cdots\cdots\cdots\cdots$$

$$\mathrm{d}_1^m a = g(a\hat{\boldsymbol{\mu}}, a^2) \tag{A4a$'$}$$

$$m\,\mathrm{d}_2\,\mathrm{d}_1^{m-1}a = g(\hat{\boldsymbol{\mu}}, a, \mathrm{d}_1a) \tag{A4b$'$}$$

$$m\,\mathrm{d}_3\,\mathrm{d}_1^{m-1}a = g(\hat{\boldsymbol{\mu}}, a, \mathrm{d}_1a, \mathrm{d}_2a) \tag{A4c$'$}$$

$$D^m a = \mathscr{L}(a\boldsymbol{\mu}, a^2; \dot{a}\boldsymbol{\mu}, a\dot{a}; \ddot{a}\boldsymbol{\mu}, a\ddot{a}, \dot{a}^2; \ldots) \tag{A5$'$}$$

Appendix B: Vectors and Matrices z and Z in Equations (12)

The vectors and matrices $\boldsymbol{z}$ and $\boldsymbol{Z}$ appearing in Eqs. (12) are obtained by solving the following linear algebraic problems.

Order ε^2:

$$\boldsymbol{F}_x^0\boldsymbol{z}_2 = -\left[\boldsymbol{F}_{xx}^0\boldsymbol{u}_1^2 - \left(\boldsymbol{v}_2^T\boldsymbol{F}_{xx}^0\boldsymbol{u}_1^2\right)\boldsymbol{u}_2\right] \tag{B1a}$$

$$\boldsymbol{F}_x^0\boldsymbol{Z}_2\boldsymbol{\mu} = -\left[\boldsymbol{F}_{x\mu}^0\boldsymbol{u}_1\boldsymbol{\mu} - \left(\boldsymbol{v}_2^T\boldsymbol{F}_{x\mu}^0\boldsymbol{u}_1\boldsymbol{\mu}\right)\boldsymbol{u}_2\right] \tag{B1b}$$

Order $\varepsilon^{5/2}$:

$$\begin{aligned}\boldsymbol{F}_x^0\boldsymbol{z}_{\frac{5}{2}} &= -\left[\boldsymbol{F}_{xx}^0\boldsymbol{u}_1\boldsymbol{u}_2 - \left(\boldsymbol{v}_2^T\boldsymbol{F}_{xx}^0\boldsymbol{u}_1\boldsymbol{u}_2\right)\boldsymbol{u}_2\right] + \left(\boldsymbol{z}_2 - \boldsymbol{v}_2^T\boldsymbol{z}_2\boldsymbol{u}_2\right)\\ \boldsymbol{F}_x^0\boldsymbol{Z}_{\frac{5}{2}}\boldsymbol{\mu} &= -\left[\boldsymbol{F}_{x\mu}^0\boldsymbol{u}_2\boldsymbol{\mu} - \left(\boldsymbol{v}_2^T\boldsymbol{F}_{x\mu}^0\boldsymbol{u}_2\boldsymbol{\mu}\right)\boldsymbol{u}_2\right] + \left[\boldsymbol{Z}_2\boldsymbol{\mu} - \boldsymbol{v}_2^T(\boldsymbol{Z}_2\boldsymbol{\mu})\boldsymbol{u}_2\right]\end{aligned} \tag{B2}$$

Order ε^3:

$$\begin{aligned}\boldsymbol{F}_x^0\boldsymbol{z}_{31} &= -\tfrac{1}{2}\left[\boldsymbol{F}_{xx}^0\boldsymbol{u}_2^2 - \left(\boldsymbol{v}_2^T\boldsymbol{F}_{xx}^0\boldsymbol{u}_2^2\right)\boldsymbol{u}_2\right] + \left(\boldsymbol{z}_{\frac{5}{2}} - \boldsymbol{v}_2^T\boldsymbol{z}_{\frac{5}{2}}\boldsymbol{u}_2\right)\\ \boldsymbol{F}_x^0\boldsymbol{z}_{32} &= \boldsymbol{z}_{\frac{5}{2}} - \boldsymbol{v}_2^T\boldsymbol{z}_{\frac{5}{2}}\boldsymbol{u}_2\\ \boldsymbol{F}_x^0\boldsymbol{z}_{33} &= -\tfrac{1}{6}\left[\boldsymbol{F}_{xxx}^0\boldsymbol{u}_1^3 - \left(\boldsymbol{v}_2^T\boldsymbol{F}_{xxx}^0\boldsymbol{u}_1^3\right)\boldsymbol{u}_2\right]\\ &\quad + \tfrac{1}{2}\left[\boldsymbol{F}_{xx}^0\boldsymbol{u}_1\boldsymbol{z}_2 - \left(\boldsymbol{v}_2^T\boldsymbol{F}_{xx}^0\boldsymbol{u}_1\boldsymbol{z}_2\right)\boldsymbol{u}_2\right]\\ \boldsymbol{F}_x^0\boldsymbol{Z}_{31}\boldsymbol{\mu} &= \boldsymbol{Z}_{\frac{5}{2}}\boldsymbol{\mu} - \left(\boldsymbol{v}_2^T\boldsymbol{Z}_{\frac{5}{2}}\boldsymbol{\mu}\right)\boldsymbol{u}_2\\ \boldsymbol{F}_x^0\boldsymbol{Z}_{32}\boldsymbol{\mu} &= -\left[\boldsymbol{F}_{xx}^0\boldsymbol{u}_1\boldsymbol{Z}_2\boldsymbol{\mu} - \left(\boldsymbol{v}_2^T\boldsymbol{F}_{xx}^0\boldsymbol{u}_1\boldsymbol{Z}_2\boldsymbol{\mu}\right)\boldsymbol{u}_2\right]\\ &\quad - \tfrac{1}{2}\left[\boldsymbol{F}_{x\mu}^0\boldsymbol{z}_2\boldsymbol{\mu} - \left(\boldsymbol{v}_2^T\boldsymbol{F}_{x\mu}^0\boldsymbol{z}_2\boldsymbol{\mu}\right)\boldsymbol{u}_2\right]\\ &\quad - \tfrac{1}{2}\left[\boldsymbol{F}_{xx\mu}^0\boldsymbol{u}_1^2\boldsymbol{\mu} - \left(\boldsymbol{v}_2^T\boldsymbol{F}_{xx\mu}^0\boldsymbol{u}_1^2\boldsymbol{\mu}\right)\boldsymbol{u}_2\right]\\ \boldsymbol{F}_x^0\boldsymbol{Z}_{33}\boldsymbol{\mu}^2 &= -\left[\boldsymbol{F}_{x\mu}^0\boldsymbol{Z}_2\boldsymbol{\mu}^2 - \left(\boldsymbol{v}_2^T\boldsymbol{F}_{x\mu}^0\boldsymbol{Z}_2\boldsymbol{\mu}^2\right)\boldsymbol{u}_2\right]\\ &\quad - \tfrac{1}{2}\left[\boldsymbol{F}_{x\mu\mu}^0\boldsymbol{u}_1\boldsymbol{\mu}^2 - \left(\boldsymbol{v}_2^T\boldsymbol{F}_{x\mu\mu}^0\boldsymbol{u}_1\boldsymbol{\mu}^2\right)\boldsymbol{u}_2\right]\end{aligned} \tag{B3}$$

Because F_x^0 is singular, the solutions to Eqs. (B1–B3) are not unique. To avoid indeterminacies, a suitable normalization condition must be enforced. If $v_1^T x = a\ \forall\varepsilon$ is required, $v_1^T x_k = 0$, $k = 1, 2, \dots,$ follows from orthonormality conditions between the left and right eigenvectors. Therefore, when Eqs. (12) are taken into account, $v_1^T z_{ij} = 0$ and $v_1^T Z_{ij} = \mathbf{0}$ must hold. These are constraint conditions for the algebraic problems (B1–B3), which remove the singularity.

Appendix C: Coefficients *h* and *k* in Equations (13)

The following scalar quantities are introduced:

$$h_1 = -v_2^T z_{\frac{5}{2}}, \qquad \boldsymbol{h}_2\boldsymbol{\mu} = -v_2^T Z_{\frac{5}{2}}\boldsymbol{\mu}, \qquad h_3 = -2v_2^T z_{31}$$

$$h_4 = -v_2^T z_{32}, \qquad \boldsymbol{h}_5\boldsymbol{\mu} = -v_2^T Z_{31}\boldsymbol{\mu}, \qquad h_6 = \tfrac{1}{2}v_2^T F_{xx}^0 u_1^2$$

$$\boldsymbol{h}_7\boldsymbol{\mu} = v_2^T F_{x\mu}^0 u_1 \boldsymbol{\mu}, \qquad h_8 = v_2^T\left(F_{xx}^0 u_1 u_2 - z_2\right)$$

$$\boldsymbol{h}_9\boldsymbol{\mu} = v_2^T\left(F_{x\mu}^0 u_2 - v_2^T Z_2\right)\boldsymbol{\mu} \tag{C1}$$

where vectors z and matrices Z are defined in Appendix B. The coefficients in Eq. (14) then are

$$\boldsymbol{k}_1\boldsymbol{\mu} = -v_2^T F_{x\mu}^0 u_1\boldsymbol{\mu}, \qquad k_2 = \tfrac{1}{2}v_2^T F_{xx}^0 u_1^2$$

$$\boldsymbol{k}_3\boldsymbol{\mu} = -v_2^T\left(F_{x\mu}^0 u_2 - Z_2\right)\boldsymbol{\mu}, \qquad k_4 = v_2^T\left(F_{xx}^0 u_1 u_2 - z_2\right)$$

$$k_5 = v_2^T\left(\tfrac{1}{2}F_{xx}^0 u_2^2 - z_{\frac{5}{2}}\right), \qquad k_6 = v_2^T\left(\tfrac{1}{2}F_{xx}^0 u_1 z_2 + \tfrac{1}{6}F_{xxx}^0 u_1^3 + h_1 h_6\right)$$

$$\boldsymbol{k}_7\boldsymbol{\mu} = v_2^T\left(F_{xx}^0 u_1 Z_2 + \tfrac{1}{2}F_{x\mu}^0 z_2 + \tfrac{1}{2}F_{xx\mu}^0 u_1^2 + \boldsymbol{h}_2 h_6 - h_1\boldsymbol{h}_7\right)\boldsymbol{\mu}$$

$$\boldsymbol{k}_8\boldsymbol{\mu}^2 = v_2^T\left(F_{x\mu}^0 Z_2 + \tfrac{1}{2}F_{x\mu\mu}^0 u_1 + \boldsymbol{h}_2\boldsymbol{h}_7\right)\boldsymbol{\mu}^2$$

$$k_9 = v_2^T\Big(F_{xx}^0 u_1 z_{\frac{5}{2}} - 3z_{33} + \tfrac{1}{2}F_{xx}^0 u_2 z_2 + \tfrac{1}{2}F_{xxx}^0 u_1^2 u_2 + h_3 h_6 + 3h_4 h_6 + h_1 h_8\Big)$$

$$\boldsymbol{k}_{10}\boldsymbol{\mu} = v_2^T\Big(F_{xx}^0 u_1 Z_{\frac{5}{2}} - 2Z_{32} + F_{xx}^0 u_2 Z_2 + F_{x\mu}^0 z_{\frac{5}{2}} + F_{xx\mu}^0 u_1 u_2 + h_3\boldsymbol{h}_7 + 2h_4\boldsymbol{h}_7 + 2\boldsymbol{h}_5 h_6 + \boldsymbol{h}_2 h_8 + h_1\boldsymbol{h}_9\Big)\boldsymbol{\mu}$$

$$\boldsymbol{k}_{11}\boldsymbol{\mu}^2 = v_2^T\left(F_{x\mu}^0 Z_{\frac{5}{2}} - Z_{33} + \tfrac{1}{2}F_{x\mu\mu}^0 u_2 + \boldsymbol{h}_5\boldsymbol{h}_7 + \boldsymbol{h}_2\boldsymbol{h}_9\right)\boldsymbol{\mu}^2 \tag{C2}$$

Appendix D: Asymptotic Expression of the Bifurcated Path and Critical Boundaries

Reconstituted steady solutions admitted to the bifurcation equation (14) are

$$a_s = 0, \qquad a_s = (1/c_2)\left(\kappa - \boldsymbol{c}_8\boldsymbol{\nu}^2 - \boldsymbol{c}_7\boldsymbol{\nu}\kappa - k_6\kappa^2\right) \tag{D1}$$

where $\boldsymbol{\nu} = \{\kappa, \xi\} \in \Re^2$, $\boldsymbol{c}_7 = \{c_{7_\kappa}, c_{7_\xi}\} \in \Re^2$, and $\boldsymbol{c}_8 = [c_{8_{ij}}] \in \Re^2 \times \Re^2$, $(i, j) = (\kappa, \xi)$, are new coefficients resulting from those in Eq. (14) after expressing the bifurcation equation as a function of the unfolding parameters $\boldsymbol{\nu}$.

The reconstituted critical boundaries for T solutions are

$$\mathcal{D}_T : \kappa = -c_{8_\xi}\xi^2$$

$$\mathcal{H}_T : \xi = -c_{11_\kappa}\kappa^2$$

$$\mathcal{N}_T : \kappa = \tfrac{1}{4}\xi^2 + \left[\left(c_{8_\kappa}/16\right)\xi^4 + \left(c_{8_{\kappa\xi}}/4\right)\xi^3 + c_{8_\xi}\xi^2\right] - \left[\left(c_{11_\kappa}/64\right)\xi^4 + \left(c_{11_{\kappa\xi}}/16\right)\xi^3 + \left(c_{11_\xi}/4\right)\xi^2\right]^2$$

The reconstituted critical boundaries for the NT steady solution are

$$\mathcal{D}_{\rm NT} : \kappa = -c_{8_\xi}\xi^2$$

$$\mathcal{H}_{\rm NT} : \xi = -(c_4/c_2)\kappa - \Big(c_{11_\kappa} + c_4 c_{11_{\kappa\xi}}/c_2 + c_4^2 c_{11_\xi}/c_2^2 + c_4 c_{8_\kappa}/c2 + c_4^2 c_{8_{\kappa\xi}}/c_2^2 + c_4^3 c_{8_\xi}/c_2^3 + c_4 c_{7_k}/c_2 + c_4 c_6/c_2 + c_4^2 c_{7_\xi}/c_2^2 - c_{10_\kappa}/c_2 - c_4 c_{10_\xi}/c_2^2 + c_9/c_2^2\Big)\kappa^2$$

$$\mathcal{N}_{\rm NT} : \kappa = -\tfrac{1}{2}[(c_4/2c_2)\xi - 1] \pm \tfrac{1}{2}\sqrt{[(c_4/2c_2)\xi - 1]^2 + \left(c_4^2/4c_2^2\right)\xi^2 + \mathcal{O}(\varepsilon^3)}$$

Acknowledgment

This research was supported by the Italian Ministry of University and Research (Cofin 2001-02 funds).

References

[1] Nayfeh, A. H., and Mook, D. T., *Nonlinear Oscillations*, Wiley, New York, 1979.

[2] Luongo, A., and Paolone, A., “On the Reconstitution Problem in the Multiple Time Scale Method,” *Nonlinear Dynamics*, Vol. 14, 1999, pp. 133–156.

[3] Sewell, M. J., “A General Theory of Equilibrium Paths Through Critical Points. I,” *Proceedings of the Royal Society of London*, 1968, pp. 201–223.

[4] Sewell, M. J., “On the Branching of Equilibrium Paths,” *Proceedings of the Royal Society of London*, 1970, pp. 499–518.

[5] Thompson, J. M. T., and Hunt, G. W., *A General Theory of Elastic Stability*, Wiley, London, 1973.

[6] Pignataro, M., Rizzi, N., and Luongo, A., *Stability, Bifurcation, and Postcritical Behavior of Elastic Systems*, Elsevier, Amsterdam, 1991.

[7] Luongo, A., and Paolone, A., “Perturbation Methods for Bifurcation Analysis from Multiple Nonresonant Complex Eigenvalues,” *Nonlinear Dynamics*, Vol. 14, 1997, pp. 193–210.

[8] Luongo, A., and Paolone, A., “Multiple Scale Analysis for Divergence-Hopf Bifurcation of Imperfect Symmetric Systems,” *Journal of Sound and Vibration*, Vol. 218, 1998, pp. 527–539.

[9] Luongo, A., Paolone, A., and Di Egidio, A., “Multiple Time Scales Analysis for 1:2 and 1:3 Resonant Hopf Bifurcations,” *Nonlinear Dynamics*, Special Issue (to be published).

[10] Luongo, A., “Eigensolutions Sensitivity for Nonsymmetric Matrices with Repeated Eigenvalues,” *AIAA Journal*, Vol. 31, 1993, pp. 1321–1328.

[11] Luongo, A., Paolone, A., and Di Egidio, A., “Sensitivities and Linear Stability Analysis Around a Double-Zero Eigenvalue,” *AIAA Journal*, Vol. 38, No. 4, 2000, pp. 702–710.

[12] Wilkinson, J. H., *The Algebraic Eigenvalue Problem*, Clarendon, Oxford, 1965.

[13] Luongo, A., Paolone, A., and Di Egidio, A., “Multiple Time Scale Analysis for Bifurcation from a Double-Zero Eigenvalue,” *Proceedings of DECT’99—1999 ASME Design Engineering Technical Conference*, American Society of Mechanical Engineers, Fairfield, NJ, Paper VIB99-8053.

[14] Maslowe, S. A., “Direct Resonance in Double-Diffusive Systems,” *Studies in Applied Mathematics*, Vol. 73, 1985, pp. 59–74.

[15] Moroz, I. M., “Amplitude Expansion and Normal Forms in a Model for Thermohaline Convection,” *Studies in Applied Mathematics*, Vol. 74, 1986, pp. 155–170.

[16] Nayfeh, A. H., “Topical Course on Nonlinear Dynamics,” *Perturbation Methods in Nonlinear Dynamics*, Società Italiana di Fisica, Santa Margherita di Pula, Italy, 1985.

[17] Guckenheimer, J., and Holmes, P., *Nonlinear Oscillations, Dynamical Systems, and Bifurcations of Vector Fields*, Springer-Verlag, New York, 1983.

[18] Iooss, G., and Joseph, D. D., *Elementary Stability and Bifurcation Theory*, Springer-Verlag, New York, 1980.

[19] Troger, H., and Steindl, A., *Nonlinear Stability and Bifurcation Theory*, Springer-Verlag, Vienna, 1991.

A. Berman
Associate Editor